Magnetophonon resonances in quasi-one-dimensional electronic systems in tilted magnetic fields

Sang Chil Lee,[1,3] Jai Yon Ryu,[1,3] Suck Whan Kim,[2] and C. S. Ting[3]
[1]*Department of Physics, Cheju National University, Cheju 690-756, Korea*
[2]*Department of Physics, Andong National University, Andong 690-756, Korea*
[3]*Texas Center for Superconductivity, University of Houston, Texas 77204*
(Received 2 September 1999; revised manuscript received 6 January 2000)

We have obtained the magnetoconductivity in quasi-one-dimensional electronic systems in tilted magnetic fields, based on a simple model of parabolic confining potentials, and investigated the qualitative features of the magnetophonon resonance (MPR) effects according to the strength of electrostatic potentials and the tilt angle of the applied magnetic field in the quantum limit condition, in which $\hbar\omega_{\pm} \gg k_B T$ are satisfied. Here ω_+ and ω_- are the effective cyclotron frequencies. In particular, the behaviors of the MPR line shape, such as the appearance of subsidiary MPR peaks, the shift of these MPR peaks, and a change in MPR amplitude and width are discussed in detail.

I. INTRODUCTION

Over the past few decades, magnetophonon resonance (MPR) effects in low-dimensional electron-gas (EG) systems have received much attention from both experimental and theoretical points of view since they can be used as an alternative magnetotransport tool for the measurement of the effective mass of quasi-two-dimensional (Q2D) electrons[1] and for the determination of the energy difference between adjacent quasi-one-dimensional (Q1D) subbands.[2] Many studies of MPR effects in such low-dimensional electronic systems have been reported.[1–15] However, most of the MPR theories presented so far are mainly restricted to the case where the magnetic field is applied normal to the interface layer of the system. Less work has been done[16] in the case where a magnetic field is applied to the Q2D electronic plane at an arbitrary angle. In this case, it is known that a suitably directed magnetic field serves to add an extra confining potential to the initial electrostatic confinement and causes a dramatic change in the energy spectrum, leading to so-called *hybrid* magnetoelectric quantization. As a consequence, one would expect different behavior of the MPR effects in such systems from the known MPR effects in three-dimensional EG systems.

Recently, Ryu, Hu, and O'Connell[16] presented the MPR conditions of Q1D systems in tilted magnetic fields, based on a simple model of parabolic confining potentials. In their study, they neglected the coupling Hamiltonian term $\sim B_x B_z xz$, since its contribution to the total electron energy is minor. This is valid for the case where the initial electrostatic confinements are stronger than the magnetic confinement. More recently, Suzuki and Ogawa[17] investigated in detail qualitative features of the MPR effects, their physical origin, and the dimensional crossover between Q2D and Q1D systems in tilted magnetic fields, based on the same model as Ryu *et al.*[16] However, their studies are confined to the weak confinement case where the electrostatic confining parameters are smaller than the cyclotron-resonance frequency. Therefore, a theory of MPR effects which is valid for the weak confinement case and the strong confinement case is needed and it is necessary to investigate various qualitative features of the MPR effects in Q1D systems, according to the strength of electrostatic potentials and the tilt angle of the applied magnetic field.

The purpose of the present work is to extend the previous results[16] by including the coupling Hamiltonian term $\sim B_x B_z xz$, to understand various qualitative behaviors of the MPR effects in Q1D electronic systems according to the strength of electrostatic potentials and the tilt angle of the applied magnetic field, and to compare our present results with the results presented by other authors. For this purpose, we shall review the conductivity σ_{yy} for Q1D electronic systems subjected to a tilted magnetic field, on the basis of the simple parabolic model for confinement potential, and we obtain MPR conditions as a function of the strength parameters (ω_1 and ω_2) of the parabolic potentials, which characterize the strength of confinement of Q1DEG. We will investigate how the MPR effects are affected by the tilt angle of applied magnetic fields and by the strengths of the confining potentials.

The rest of the paper is organized as follows. In Sec. II, we review an exactly solvable model for Q1D electronic systems. General formulas of the transverse magnetoconductivity σ_{yy} for the Q1D systems are presented in Sec. III, where the conductivity consists of the usual Drude term arising from the drift motion of electrons and hopping terms associated with MPR. The relaxation rate, which is closely related to the MPR, is evaluated for the quantum limit condition, assuming that the interaction with a bulk longitudinal-optical (LO) phonon is the dominant scattering mechanism. Numerical results of magnetoconductivity for the Q1D systems are presented in Sec. IV. In particular, the MPR conditions for the model system are given explicitly and the effects of tilted magnetic fields and the confining potential on the MPR are discussed. Here, special attention is given to the behavior of the MPR line shape, such as the appearance of subsidiary MPR peaks, the shift of these MPR peaks, and a change in MPR amplitude and width. Concluding remarks will be given in the final section.

II. MODEL FOR Q1D ELECTRONIC SYSTEMS IN TILTED MAGNETIC FIELDS

We consider the transport of an electron gas in a quantum-wire structure as treated by Ihm *et al.*[18] The Q2D electron gas is assumed to be confined to the x-y plane by an ideal parabolic potential $\frac{1}{2}m^*\omega_2^2 z^2$, whereas the Q1D electron gas is assumed to be further confined in the x direction by an additional parabolic potential $\frac{1}{2}m^*\omega_1^2 x^2$, thus restricting free motion to the y axis alone. In the presence of a magnetic field, the one-particle Hamiltonian (h_e) for such Q1D electrons is expressed in a unified manner by

$$h_e=\frac{1}{2m^*}(\mathbf{p}+e\mathbf{A})^2+\frac{1}{2}m^*\omega_1^2x^2+\frac{1}{2}m^*\omega_2^2z^2, \qquad (1)$$

where $\mathbf{A}$ is a vector potential accounting for a constant magnetic field $\mathbf{B}=\nabla\times\mathbf{A}$ and m^* is the effective mass. We can see the dimensional crossover between the Q2D and the Q1D electronic systems (i.e., $\omega_1\to 0$ or $\omega_2\to 0$ for the Q2D electronic system) as well as the difference in the strength of each confinement by varying the confining potential parameters (ω_1 and ω_2) in Eq. (1) for the Q1D systems. We shall consider the case where the magnetic field $\mathbf{B}$ is applied in the transverse tilt direction to the wire of the system: $B=(B_x,0,B_z)=(B\sin\theta,0,B\cos\theta)$, with the Landau gauge $\mathbf{A}=(0,xB_z-zB_x,0)$. Here the angle θ is measured from the z axis in the x-z plane. Then, the one-particle Hamiltonian (1) for those confined (Q1D) electrons subject to the transverse tilted magnetic field can be represented in the new Cartesian coordinates (x',y',z') as

$$h_e=\frac{P_{x'}^2}{2m^*}+\frac{P_{z'}^2}{2m^*}+\frac{1}{2}m^*\Omega_1^2x'^2+\frac{1}{2}m^*\Omega_2^2z'^2-m^*\omega_x\omega_z x'z'+\frac{P_{y'}^2}{2\tilde{m}^*}, \qquad (2)$$

which represents two coupled harmonic oscillators, where $\omega_x=\omega_c\sin\theta$, $\omega_z=\omega_c\cos\theta$, $\omega_c=eB/m^*$, $\tilde{m}^*=m^*(\Omega_1^2\Omega_2^2-\omega_x^2\omega_z^2)/\omega_1^2\omega_2^2$, $\Omega_1^2=\omega_1^2+\omega_z^2$, and $\Omega_2^2=\omega_2^2+\omega_x^2$. To obtain Eq. (2), we performed the following unitary transformation: $x_i'=U_1x_iU_1^{-1}$ and $P_{x_i'}=U_1P_{x_i}U_1^{-1}$ for an arbitrary x_i ($x_i=x$, y, and z for $i=1$, 2, and 3, respectively). Here $U_1=\exp[iG_1/\hbar]$ is a unitary operator with $G_1=\omega_zP_yP_x/(\tilde{m}^*\omega_1^2)-\omega_xP_zP_y/(\tilde{m}^*\omega_2^2)$.

For the purpose of diagonalizing the one-particle Hamiltonian given by Eq. (2), we take into account another unitary transformation: $X_i=U_2x_i'U_2^{-1}$ and $P_{X_i}=U_2P_{x_i'}U_2^{-1}$ for an arbitrary x_i' ($x_i'=x'$, y', and z' for $i=1$, 2, and 3, respectively), where $U_2=\exp[iG_2/\hbar]$ is a unitary operator having $G_2=\{x'P_{z'}-z'P_{x'}\}\phi$ with $\phi=\arctan\{\Omega_2^2-\omega_-^2/(\Omega_1^2-\omega_-^2)\}$. Here ω_- is the effective cyclotron frequency in the Z direction. Then, Eq. (2) can be expressed in the simplified manner as

$$h_e=\frac{1}{2m^*}P_X^2+\frac{1}{2m^*}P_Z^2+\frac{1}{2m^*}\omega_+^2X^2+\frac{1}{2m^*}\omega_-^2Z^2+\frac{1}{2\tilde{m}^*}P_Y^2, \qquad (3)$$

where ω_+^2 and ω_-^2 are, respectively, given by $\omega_\pm^2=\frac{1}{2}[\Omega_1^2+\Omega_2^2\pm\sqrt{(\Omega_1^2-\Omega_2^2)^2+4\omega_x^2\omega_z^2}]$. The Hamiltonian (3) represented in the new Cartesian coordinates is basically changed into the Hamiltonian for two independent 1D simple harmonic oscillators, one with the effective cyclotron frequency ω_+ in the X direction and the other with the effective cyclotron frequency ω_- in the Z direction. The last term in Eq. (3) denotes the y-component kinetic energy of a confined electron with a field-dependent renormalized mass $\tilde{m}^*$ with respect to the effective mass m^*. In particular, the effective mass $\tilde{m}^*$ is influenced by a factor $(\Omega_1^2\Omega_2^2-\omega_x^2\omega_z^2)/\omega_1^2\omega_2^2$, which depends on a tilt angle θ, the cyclotron frequency ω_c, and the confining potential parameters (ω_1,ω_2) characterizing the dimensionality of the system. The momentum component $P_y(=P_Y)$ is a constant of motion and can be written as $P_Y=\hbar k_Y$, where k_Y is the quasicontinuous wave vector of motion parallel to the interfaces [viz., wire in the $y(=Y)$ direction].

The normalized eigenfunctions and eigenenergies of the one-electron Hamiltonian (3) are given by

$$\langle\mathbf{R}|\lambda\rangle\equiv\langle X,Y,Z|n,l,k_y\rangle=\left(\frac{1}{L_y}\right)^{1/2}\Psi_n(X)\Psi_l(Z)\exp(ik_yY) \qquad (4)$$

and

$$E_\lambda\equiv E_{n,l}(k_y)=(n+1/2)\hbar\omega_++(l+1/2)\hbar\omega_-+\frac{(\hbar k_y)^2}{2\tilde{m}^*}, \quad n,l=0,1,2,\ldots, \qquad (5)$$

respectively. In Eq. (4), $\Psi_n(X)$ and $\Psi_l(Z)$ denote 1D simple-harmonic-oscillator wave functions. The state of the Q1D system is specified by two Landau-level indices n,l, and the wave function $\exp(ik_yy)$ in Eq. (4) expresses a free motion in the y (i.e., Y) direction. As shown in Eq. (5), the energy spectrum for the present Q1D system is *hybrid*-quantized due to the presence of the tilted magnetic field. The set of quantum numbers is designated by (n,l,k_y), where n and l denote the effective Landau (magnetic) level indices. We note that the dimensional crossover can be seen in the energy spectrum by simply varying the confining potential parameters; ω_1 or $\omega_2\to 0$ for the Q2DEG system and ω_1 and $\omega_2\to 0$ for the 3DEG system.

III. MAGNETOCONDUCTIVITY ASSOCIATED WITH RELAXATION RATES

In this section, we want to evaluate an analytical expression of the transverse magnetoconductivity σ_{yy} for the Q1D systems previously described, by taking the real part of a general expression for the complex nonlinear dc conductivity $\tilde{\sigma}_{kl}(E)$ $(k,l=x,y,z)$ given in Ref. 19 and the linear-response

limit, i.e., $\lim_{E\to 0}\mathrm{Re}\{\tilde{\sigma}_{kl}(E)\}\equiv\sigma_{kl}$. The dc linear conductivity for weak electric fields is obtained by the sum of the nonhopping part σ_{yy}^{nh} and the hopping part σ_{yy}^{h}, which are

$$\sigma_{yy}^{nh}=\frac{\hbar^3\beta e^2}{\tilde{m}^{*2}V}\sum_{n,l,k_y}k_y^2 f(E_{nl}(k_y))\times[1-f(E_{nl}(k_y))]/\tilde{\Gamma}(n,l,k_y;n,l,k_y), \tag{6}$$

$$\sigma_{yy}^{h}=\frac{e^2\omega_z^2 l_+^2}{V\omega_+}\sum_{n,l,k_y}(n+1)[f(E_{nl}(k_y))-f(E_{n+1l}(k_y))]\times\frac{\tilde{\Gamma}(n+1,l,k_y;n,l,k_y)}{(\hbar\omega_+)^2+\tilde{\Gamma}^2(n+1,l,k_y;n,l,k_y)}+\frac{e^2\omega_x^2 l_-^2}{V\omega_-}\sum_{n,l,k_y}(l+1)[f(E_{nl}(k_y))-f(E_{nl+1}(k_y))]\times\frac{\tilde{\Gamma}(n,l+1,k_y;n,l,k_y)}{(\hbar\omega_-)^2+\tilde{\Gamma}^2(n,l+1,k_y;n,l,k_y)}, \tag{7}$$

for the shift zero in the spectral line shape, where $V=L_xL_yL_z$ is the volume of the system and $\beta=1/k_BT$ with k_B being the Boltzmann constant and T temperature. Also, $l_\pm=\sqrt{\hbar/m^*\omega_\pm}$, $\hbar$ is the Planck constant divided by 2π, $f(E_{nl}(k_y))$ is a Fermi-Dirac distribution function for electrons with the eigenstate $|n,l,k_y\rangle$ of Eq. (4) and the energy $E_{nl}(k_y)$ of Eq. (5), and $-e(<0)$ is the electron charge. The quantity $\tilde{\Gamma}$ given in Eqs. (6) and (7), which appears in terms of the collision broadening due to the electron-background (phonon or impurity) interaction, plays the role of the relaxation rate in the spectral line shape. To obtain Eqs. (6) and (7), we used the matrix elements $|\langle k_y,l,n|j_Y|k_y',l',n'\rangle|^2$ given by

$$|\langle k_y,l,n|j_Y|k_y',l',n'\rangle|^2=(e\hbar k_y/\tilde{m}^*)^2\delta_{nn'}\delta_{ll'}\delta_{k_yk_y'}+(e\omega_z l_+/\sqrt{2})^2\times[n\delta_{n'n-1}+(n+1)\delta_{n'n+1}]\delta_{ll'}\delta_{k_yk_y'}+(e\omega_x l_-/\sqrt{2})^2[l\delta_{l'l-1}+(l+1)\delta_{l'l+1}]\delta_{nn'}\delta_{k_yk_y'}, \tag{8}$$

where the Kronecker symbols ($\delta_{n'n}$, $\delta_{l'l}$, $\delta_{k_yk_y'}$) denote the selection rules, which arise during the integration of the matrix elements with respect to each direction. Equation (6) expresses the Drude term arising from the drift (nonhopping) motion of electrons within the localized states through the electron-phonon interaction. In contrast, Eq. (7) expresses the hopping terms, which are associated with electron hopping motion between the localized (effective Landau and/or subband) states by absorbing and/or emitting a phonon with an energy $\hbar\omega_{\mathbf{q}}$ in the scattering events. In fact, these terms are related to the oscillatory behavior of MPR effects. Accordingly, hereafter we shall denote the transverse magnetoconductivity associated with these hopping terms as $\sigma_{yy}^{\mathrm{MPR}}$. As shown in Eq. (7), the electronic transport properties (e.g., electronic relaxation processes, magnetophonon resonances, etc.) in the Q1D systems can be studied by examining the behavior of $\tilde{\Gamma}$ as a function of the relevant physical parameters introduced in the theory.

An analytical expression of the relaxation rate in the lowest-order approximation for the weak electron-phonon interaction and in the limit of weak electric fields can be evaluated from the general expression of the electric-field-dependent relaxation rate given by Eq. (4.39) of Ref. 19. The Q1D version of the relaxation rate associated with the electronic transition between the states $|n_1,l_1,k_{1y}\rangle$ and $|n,l,k_y\rangle$ is expressed by

$$\tilde{\Gamma}(n_1,l_1,k_{1y};n,l,k_y)=\frac{D'}{4\pi^2 l_+ l_-}\sum_{(n',l')\neq(n_1,l_1)}F_{n_1n'}(\Delta n)F_{l_1l'}(\Delta l)\int_{-\infty}^{\infty}dq_Y\{(N_0+1)\delta[(n-n')\hbar\omega_+ +(l-l')\hbar\omega_- +S(k_y,k_y')-\hbar\omega_L]+N_0\delta[(n-n')\hbar\omega_+ +(l-l')\hbar\omega_- +S(k_y,k_y')+\hbar\omega_L]\}+\frac{D'}{4\pi^2 l_+ l_-}\sum_{(n',l')\neq(n,l)}F_{n'n}(\Delta n)F_{l'l}(\Delta l)\int_{-\infty}^{\infty}dq_Y\{(N_0+1)\delta[(n'-n_1)\hbar\omega_+ +(l'-l_1)\hbar\omega_- +S(k_y',k_{1y})+\hbar\omega_L]+N_0\delta[(n'-n_1)\hbar\omega_+ +(l'-l_1)\hbar\omega_- +S(k_y',k_{1y})-\hbar\omega_L]\} \tag{9}$$

with $S(k_y,k_y')=\hbar^2(k_y^2-k_y'^2)/2\tilde{m}^*$ and $S(k_y',k_{1y})=\hbar^2(k_y'^2-k_{1y}^2)/2\tilde{m}^*$, where N_0 is the optical-phonon distribution function given by $N_{\mathbf{q}}=[\exp(\beta\hbar\omega_{\mathbf{q}})-1]^{-1}$ with $\omega_{\mathbf{q}}=\omega_L$, and n' and l' indicate the intermediate localized Landau-level indices. In order to obtain the relaxation rates $\tilde{\Gamma}$ of Eq. (9) for a specific electron-phonon interaction, we considered the Fourier component of the interaction potential[8,16,17] for optical-phonon scattering given by D'/V with $D'=\hbar D^2/2\rho\omega_L\approx$const, D being a constant and ρ being the density, where the assumption was made that the phonons are dispersionless (i.e., $\hbar\omega_{\vec{q}}\approx\hbar\omega_L\approx$const, where ω_L is the optical-phonon frequency) and bulk (i.e., three-dimensional). We also took into account the following matrix element in the representation (4):

$$|\langle n,l,k_y|U\exp(\pm i\vec{q}\cdot\vec{r})U^{-1}|n',l',k_y'\rangle|^2 = |J_{nn'}(u_+)|^2|J_{ll'}(u_-)|^2\delta_{k_y',k_y\mp q_y}, \tag{10}$$

$$|J_{nn'}(u)|^2=\frac{n_<!}{n_>!}e^{-u}u^{\Delta n}[L_{n_>}^{\Delta n}(u)]^2, \tag{11}$$

where $n_<=\min\{n,n'\}$, $n_>=\max\{n,n'\}$, $u_+=l_+^2q_X^2/2$, $u_-=l_-^2q_Z^2/2$, and $L_{n<}^{\Delta n}(u)$ is an associated Laguerre polynomial[20] with $\Delta n=n_>-n_<$. In addition, we utilized the following relation in doing the integral over q_X and q_Z:

$$F_{n'n}(\Delta n)\equiv\int_0^\infty\frac{1}{\sqrt{u}}|J_{n'n}(u)|^2du = \frac{n_<!}{n_>!}\frac{(1+\Delta n)_{n_<}(2\Delta n+\frac{3}{2})_{n_<}\Gamma(\Delta n+\frac{1}{2})}{(n_<!)^2} \times{}_3\Phi_2(-n_<,\Delta n+\tfrac{1}{2},\tfrac{1}{2};\Delta n+1,\tfrac{1}{2}-n_<;1). \tag{12}$$

Here ${}_3\Phi_2(a,b,c;d,e;x)$ is the hypergeometric function[20]

$${}_3\Phi_2(a,b,c;d,e;x)=\sum_{n=0}^{\infty}\frac{(a)_n(b)_n(c)_n}{(d)_n(e)_n}\frac{x^n}{n!} \tag{13}$$

with Pochhammer's symbol $(a)_n$ defined by $(a)_n=a(a+1)\cdots(a+n-1)=\Gamma(a+n)/\Gamma(a)$. It should be noted that the Landau-level indices n_1 and l_1 given in Eq. (9) are, respectively, replaced by $n+1$ and l or n and $l+1$ for the electron hopping motion, de pending on the type of the transitions associated with the Landau-level index, and that the summations of Eq. (9) over the Landau level can be, respectively, divided into two possible cases: (i) $\Sigma_{n'\neq n_1}\Sigma_{l'}$ and $\Sigma_{n'\neq n}$, $\Sigma_{l'}$, and (ii) $\Sigma_{n'}\Sigma_{l'\neq l_1}$ and $\Sigma_{n'}\Sigma_{l'\neq l}$ since the condition $(n',l')\neq(n_1,l_1)$ in the summation of Eq. (9) contains three types of contributions: (i) $n'\neq n_1$, $l'\neq l_1$; (ii) $n'\neq n_1$, $l'=l_1$; and (iii) $n'=n_1$, $l'\neq l_1$. The δ functions in Eq. (9) express the law of energy conservation in one-phonon collision (absorption and emission) processes. The strict energy-conserving δ functions in Eq. (9) imply that when the electron undergoes a collision by absorbing energy from the field, its energy can only change by an amount equal to the energy of a phonon involved in the transitions. This in fact leads to magnetophonon resonance effects due to the Landau levels.

Now, let us consider the case where the nondegenerate limit and the quantum limit ($\hbar\omega_+,\hbar\omega_-\gg k_BT$) are satisfied so that the electrons can be in the lowest Landau levels (viz., $n=0$ and $l=0$). Then, the transverse magnetoconductivity of Eq. (7) for the electron hopping motion due to the Landau-level indices n and l can be expressed by

$$\sigma_{yy}^{\rm MPR}\approx n_ee^2\sqrt{\frac{\beta^3\hbar^6}{2\tilde{m}^{*3}\pi}}\frac{\omega_z^2l_+^2}{\omega_+}\{1-\exp(-\beta\hbar\omega_+)\}\int dk_y \times\exp\left[-\beta\frac{(\hbar k_y)^2}{2\tilde{m}^*}\right]\frac{\tilde{\Gamma}(1,0,k_y;0,0,k_y)}{(\hbar\omega_+)^2+\tilde{\Gamma}^2(1,0,k_y;0,0,k_y)} + n_ee^2\sqrt{\frac{\beta^3\hbar^6}{2\tilde{m}^{*3}\pi}}\frac{\omega_x^2l_-^2}{\omega_-}\{1-\exp[-\beta\hbar\omega_-]\} \times\int dk_y\exp\left(-\beta\frac{(\hbar k_y)^2}{2\tilde{m}^*}\right) \times\frac{\tilde{\Gamma}(0,1,k_y;0,0,k_y)}{(\hbar\omega_-)^2+\tilde{\Gamma}^2(0,1,k_y;0,0,k_y)}, \tag{14}$$

where $n_e=N_e/V$ is the electron density with $N_e=\sqrt{2\tilde{m}^*L_y^2/\beta\pi\hbar^2}\exp[\beta\{E_F-\hbar(\omega_++\omega_-)/2\}]$. To obtain the dc magnetoconductivity of Eq. (14) in simpler form, we assumed that the f's in Eq. (7) are replaced by the Boltzmann distribution function for nondegenerate semiconductors,[12,14,16,17] i.e., $f(E_{n,l}(k_y))\approx\exp\{\beta[E_F-E_{nl}(k_y)]\}$, where E_F denotes the Fermi energy. We also replaced one summation with respect to k_y in Σ_{n,l,k_y} by the following relation:[12,14,16,17] $\Sigma_{k_y}(\cdots)\rightarrow(L_y/2\pi)\int_{-\infty}^{\infty}dk_y(\cdots)$. In the case where the quantum limit ($\hbar\omega_+,\hbar\omega_-\gg k_BT$) is satisfied, only one or two Landau levels are customarily occupied. Accordingly, it may be sufficient for us to consider the electronic transitions between the states specified by $n_i=0,1$ and $l_i=0,1$ ($i=1,2$) in Eq. (9) for the fundamental MPR. Then, the relaxation rates of Eq. (9) for the electron hopping motion due to the Landau-level indices n and l are, respectively, given, after the q_Y integration, by

$$\tilde{\Gamma}(1,0,k_y;0,0,k_y)=N_0\Lambda\left\{\frac{1}{\sqrt{|2\tilde{m}^*\{\hbar\omega_--\hbar\omega_L\}/\hbar^2-k_y^2|}} + \frac{(3/4)}{\sqrt{|2\tilde{m}^*\{\hbar\omega_++\hbar\omega_--\hbar\omega_L\}/\hbar^2-k_y^2|}} + \frac{1}{\sqrt{|2\tilde{m}^*\{\hbar\omega_--\hbar\omega_+-\hbar\omega_L\}/\hbar^2-k_y^2|}}\right\}, \tag{15}$$

$$\tilde{\Gamma}(0,1,k_y;0,0,k_y)=N_0\Lambda\left\{\frac{1}{\sqrt{|2\tilde{m}^*\{\hbar\omega_+-\hbar\omega_L\}/\hbar^2-k_y^2|}} + \frac{(3/4)}{\sqrt{|2\tilde{m}^*\{\hbar\omega_++\hbar\omega_--\hbar\omega_L\}/\hbar^2-k_y^2|}} + \frac{1}{\sqrt{|2\tilde{m}^*\{\hbar\omega_+-\hbar\omega_--\hbar\omega_L\}/\hbar^2-k_y^2|}}\right\}, \tag{16}$$

where $\Lambda = D' \tilde{m}^* / 4\pi l_+ l_- \hbar^2$. Note that we considered only the phonon absorption process since we are interested in the physical properties of MPR in a specific process. As can be seen from Eqs. (14)–(16), the relaxation rates play an important role to determine the height and width of the MPR peaks as well as their peak positions. Equation (14), supplemented by Eqs. (15) and (16), is the basic equation for the MPR spectral line shape arising from the electron hopping motion between the effective Landau states by absorbing a phonon with an energy $\hbar\omega_{\mathbf{q}}$ in the scattering events, which enables us to analyze MPR effects in the Q1D electronic systems under tilted magnetic fields.

IV. NUMERICAL RESULTS AND DISCUSSION

In this section we present the numerical results of the magnetoconductivity formula $\sigma_{yy}^{\mathrm{MPR}}$ in Eq. (14), which is related to the MPR for the Q1D electronic systems based on the model described in Sec. II. Here, special attention is given to the behavior of the MPR line shape, such as the appearance of subsidiary MPR peaks, the shift of these MPR peaks, and a change in MPR amplitude and width. For our numerical results of Eq. (14), we consider the Q1D electronic systems with effective mass $m^* = 0.067 m_0$ with m_0 being the electron rest mass and LO-phonon energy $\hbar\omega_L = 36.6$ meV as an example. The sample temperature is assumed to be 50 K in this calculation. The quantity D' in Eq. (16) is taken by 4.11×10^{-68} $\mathrm{kg^2\,m^7\,s^{-4}}$.[21,22] Figure 1 shows the spectral line shapes of $\sigma_{yy}^{\mathrm{MPR}}$ for the Q1D system as a function of magnetic field B for various tilt angles θ of the transverse tilted magnetic field $B = (B \sin\theta, 0, \cos\theta)$ applied to the electronic wire, where we considered three cases for confinement frequencies ω_1 and ω_2 in the x and z direction: (a) $\omega_1 = 0.2\omega_L$ and $\omega_2 = 0.5\omega_L$, (b) $\omega_1 = 0.5\omega_L$ and $\omega_2 = 0.2\omega_L$, and (c) $\omega_1 = \omega_2 = 0.2\omega_L$, as an example, in order to see the effect of tilted magnetic fields, viz., θ dependency of MPR depending on the condition of the confining potential parameters. Moreover, to understand the effect of electrostatic confining potentials (characterized by ω_1, ω_2) on MPR, we plotted the spectral line shapes of $\sigma_{yy}^{\mathrm{MPR}}$ for the Q1D system in Fig. 2, as a function of magnetic field B for various confining potential parameters at a fixed angles θ, where the tilt angle was taken as 30° as a matter of convenience. In these figures, we can see the following features for the Q1D system: (i) there are three peaks in the $\sigma_{yy}^{\mathrm{MPR}}$ under the magnetic field up to 40 Tesla; (ii) the shift of the resonant peaks in the conductivity for $\omega_1 \neq \omega_2$ corresponding to an asymmetric quantum wire is very sensitive to the tilt angle θ of applied magnetic field and the relative strength of the confining potential parameters ω_1 and ω_2 in the x and z direction, while for $\omega_1 = \omega_2$ corresponding to a symmetric quantum wire, it does not depend on the tilt angle; and (iii) the height of these peaks and their resonance widths are closely related to the tilt angle θ and the confining potential parameters ω_1 and ω_2.

Let us first examine feature (i). Since MPR is a phenomenon which occurs in the electronic system subjected to quantizing magnetic fields, the resonant transition in the Q1D electronic structure under tilted magnetic fields takes place in terms of the Landau-level indices n and l, whereby

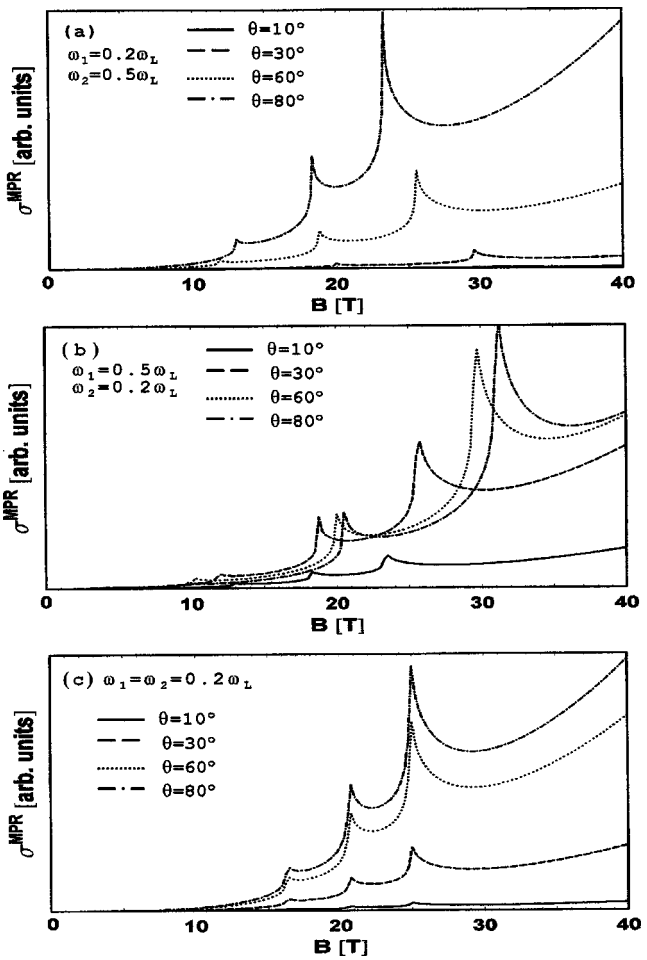

FIG. 1. Magnetic field (B) dependence of the magnetoconductivity ($\sigma_{yy}^{\mathrm{MPR}}$) for different tilt angles (θ's): (a) $\omega_1 = 0.2\omega_L$, $\omega_2 = 0.5\omega_L$, (b) $\omega_1 = 0.5\omega_L$, $\omega_2 = 0.2\omega_L$, and (c) $\omega_1 = \omega_2 = 0.2\omega_L$.

$\hbar\omega_+, \hbar\omega_- \gg \tilde{\Gamma}$ are satisfied. In this case, the abrupt change of the relaxation time (and hence magnetoconductivity) is expected to occur at the resonant magnetic field when we vary the strength and/or the tilt angle θ of the applied magnetic field. As can be seen from Eqs. (14)–(16), there are four possible cases which change $\tilde{\Gamma}$ abruptly under the condition that the density of states is maximum (i.e., at $k = 0$): $\hbar\omega_- = \hbar\omega_L$, $\hbar\omega_+ + \hbar\omega_- = \hbar\omega_L$, $\hbar\omega_+ = \hbar\omega_L$, and $\hbar\omega_+ - \hbar\omega_- = \hbar\omega_L$, which are the conditions for MPR giving the peak positions (i.e., resonant magnetic fields) in the spectral line shape, because the condition $\hbar\omega_- - \hbar\omega_+ = \hbar\omega_L$ is obviously impossible from the definition of the effective frequencies ω_+ and ω_-. It is to be noted that the MPR conditions are sensitive to the confining potential parameters (ω_1 and ω_2). For given ω_1 and ω_2 in Figs. 1 and 2, the resonant behaviors are actually given by the following three cases:

$$\hbar\omega_+ + \hbar\omega_- = \hbar\omega_L, \quad \hbar\omega_+ = \hbar\omega_L, \quad \hbar\omega_+ - \hbar\omega_- = \hbar\omega_L \tag{17}$$

under the magnetic field up to 40 Tesla. In the course of scattering events, the electrons in the effective Landau and subband levels specified by the level indices (n,l) could make transitions to one of the effective Landau and subband levels (n',l') by absorbing a LO-phonon energy $\hbar\omega_L$ when

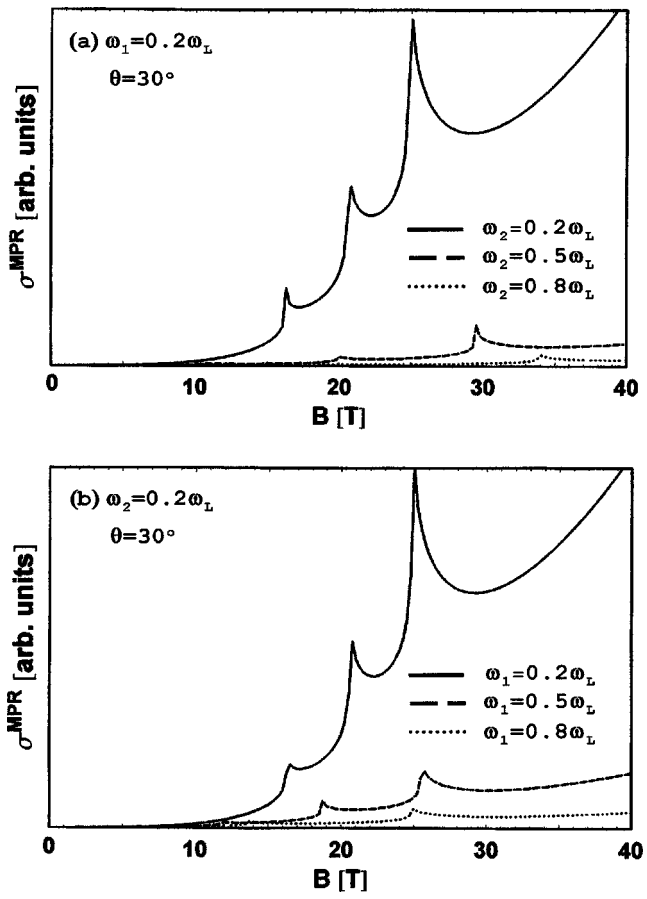

FIG. 2. Magnetic field (B) dependence of the magnetoconductivity ($\sigma_{yy}^{\mathrm{MPR}}$) for (a) the change of the confining potential strength ω_2 in the z direction and (b) the change of the confining potential strength ω_1 in the x direction.

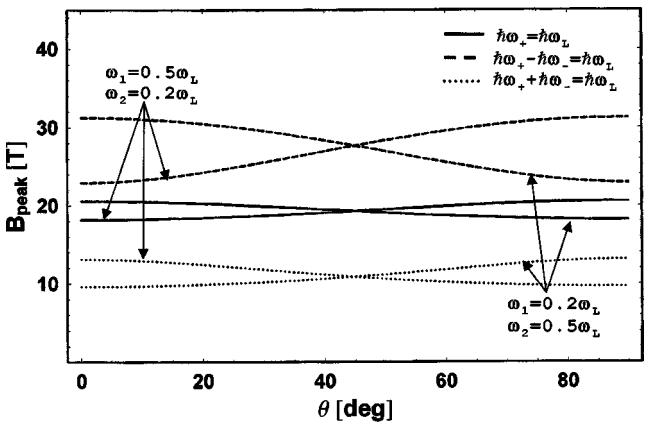

FIG. 3. Tilt angle dependence of the resonant magnetic fields (B_{peak}), viz., the MPR peak positions for $\omega_1=0.2\omega_L$, $\omega_2=0.5\omega_L$ and $\omega_1=0.5\omega_L$, $\omega_2=0.2\omega_L$. The solid, dashed, and dotted lines correspond to $\hbar\omega_+=\hbar\omega_L$, $\hbar\omega_+-\hbar\omega_-=\hbar\omega_L$, and $\hbar\omega_++\hbar\omega_-=\hbar\omega_L$, respectively.

the conditions (17) are satisfied. The first condition indicates a process corresponding to the electronic transition from $(n,l)=(0,0)$ to $(1,1)$, where quasielectrons having respective energy of $\hbar\omega_+$ and $\hbar\omega_-$ are created by absorbing a LO phonon with energy $\hbar\omega_L$. The second condition indicates a process corresponding to the electronic transition either from $(0,0)$ to $(1,0)$ or from $(0,1)$ to $(1,1)$, where only a quasielectron with energy $\hbar\omega_+$ is created by absorbing the same phonon energy. The third condition indicates a process corresponding to the electronic transition from $(0,1)$ to $(1,0)$, where, by absorbing a LO phonon with the same energy, a quasielectron with $\hbar\omega_+$ is created and a quasielectron with energy $\hbar\omega_-$ is, however, annihilated. It is shown from Eq. (17) that additional MPR conditions (subsidiary peaks) appear at $\hbar\omega_+\pm\hbar\omega_-=\hbar\omega_L$ on both sides of the MPR peaks at $\hbar\omega_+=\hbar\omega_L$. The origin of the appearance of the subsidiary peaks in the Q1D systems is mainly due to the presence of the effective confining potential $m\omega_-^2Z^2/2$, i.e., ω_- in Eq. (17), which is unlike the MPR in a 3D electronic system (where only one resonant peak appears at $\hbar\omega_+=\hbar\omega_c=\hbar\omega_L$ when $P=1$; here P is the difference of Landau-level index).[23–26] Thus, the appearance of these subsidiary peaks in the MPR line shape seems to be a characteristic feature in Q1D electronic systems. If the frequencies ω_+ and ω_- in Eq. (17) are replaced by Ω_1 and Ω_2, respectively, Eq. (17) is reduced to our previous result[16] for a Q1D quantum-wire structure modeled by the same potential wells, which is valid for the strong confinement potentials with respect to the cyclotron-resonance frequency. Moreover, if the frequencies ω_+ and ω_- in Eq. (17) are replaced by $\sqrt{\omega_1^2\cos^2\theta+\omega_2^2\sin^2\theta+\omega_c^2}$ and $\sqrt{\omega_1^2\sin^2\theta+\omega_2^2\cos^2\theta}$, respectively, Eq. (17) is reduced to the result of Suzuki *et al.*[17] for a Q1D quantum-wire structure modeled by the same potential wells, which is valid for weak confinement potentials.

Next, let us pay attention to the shift of the resonant peaks in the conductivity seen in Figs. 1 and 2, which is related to feature (ii). Their shift in the conductivity can be understood in terms of the behaviors of $\hbar\omega_+$ and $\hbar\omega_+\pm\hbar\omega_-$ in Eq. (17) since the quantities $\hbar\omega_+$ and $\hbar\omega_+\pm\hbar\omega_-$ intercept $\hbar\omega_L$ at the resonant magnetic-field values. The quantities $\hbar\omega_+$ and $\hbar\omega_+\pm\hbar\omega_-$ are mainly influenced by the tilt angle of the applied magnetic field and the strength of the confining potential parameters (ω_1,ω_2). Therefore, we will concentrate on how MPR peaks change according to these factors. Figure 3 shows the shift of resonant peaks in the conductivity seen in Fig. 1 as a function of tilt angle θ depending on the confinement conditions given in Fig. 1. As can be seen from the figure, in the case of $\omega_1<\omega_2$, the resonant point for the subsidiary peak in the low field side determined from the condition $\hbar\omega_++\hbar\omega_-=\hbar\omega_L$ shifts to the corresponding point in the higher field side. Those resonant points for the central peak given by $\hbar\omega_+=\hbar\omega_L$ and for the subsidiary peak in the high field side given by $\hbar\omega_+-\hbar\omega_-=\hbar\omega_L$ shift to the corresponding points in the lower field side, respectively, as the tilt angle is increased, which has an identical behavior to that reported by Suzuki *et al.*[17] However, the shift of the resonant peaks for $\omega_1>\omega_2$ is contrary to that for $\omega_1<\omega_2$. In other words, for $\omega_1>\omega_2$, the peak in the low field side of the magnetic field shifts to the lower field side whereas the peaks in the middle and the high field side of the field shift to the higher field side, as the tilt angle θ of the applied magnetic field is increased. It is noted that our present results do not agree with the experimental results of Brummell *et al.*[6] for Q2D electronic systems, indicating that all of the MPR peaks shift to the higher B side. As mentioned by Suzuki *et al.*,[17] this disagreement may be due to the fact that their experiment was performed under the magnetic

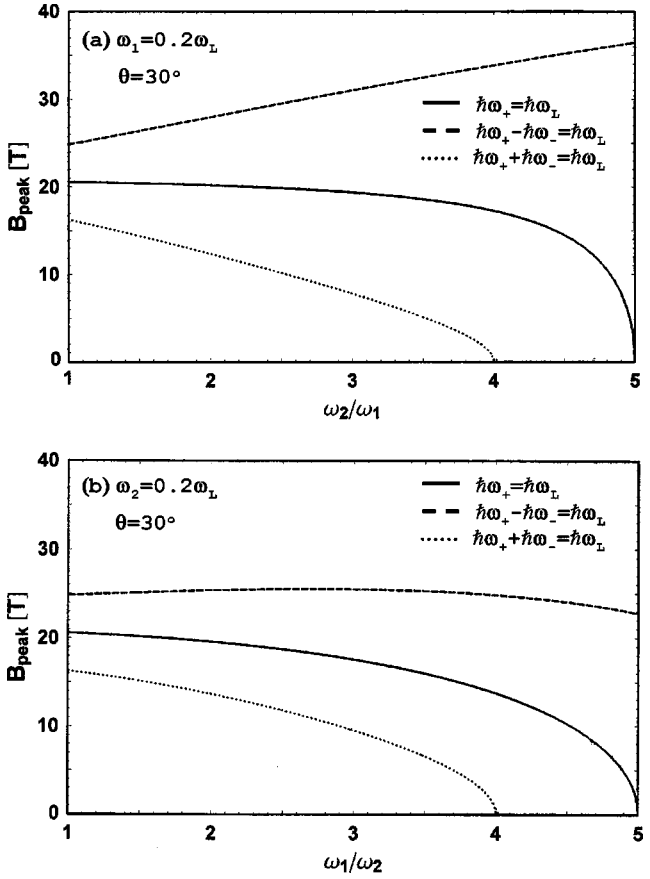

FIG. 4. Relative confining potential strength dependence of the resonant magnetic fields (B_{peak}) at a fixed angle $\theta=30°$: (a) $\omega_1=0.2\omega_L$ and (b) $\omega_2=0.2\omega_L$. The solid, dashed, and dotted lines indicate $\hbar\omega_+=\hbar\omega_L$, $\hbar\omega_+-\hbar\omega_-=\hbar\omega_L$, and $\hbar\omega_++\hbar\omega_-=\hbar\omega_L$, respectively.

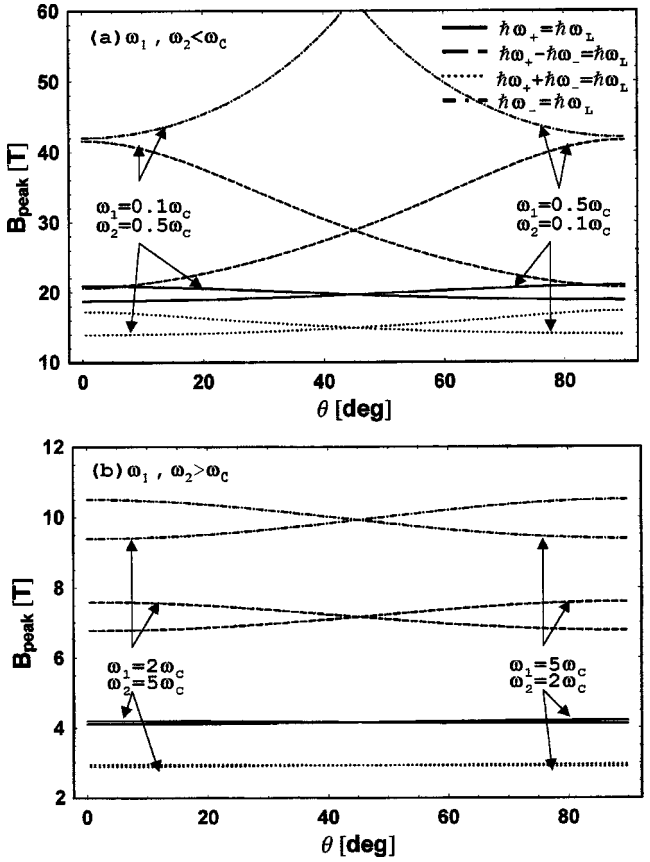

FIG. 5. Tilt angle dependence of the resonant magnetic fields (B_{peak}): (a) $\omega_1,\omega_2<\omega_c$ and (b) $\omega_1,\omega_2>\omega_c$, where ω_1 and ω_2 have been taken as $0.1\omega_c$ or $0.5\omega_c$ for weak confinements and as $2\omega_c$ or $5\omega_c$ for strong confinements. The solid, dashed, dotted, and dashed-dotted lines correspond to $\hbar\omega_+=\hbar\omega_L$, $\hbar\omega_+-\hbar\omega_-=\hbar\omega_L$, $\hbar\omega_++\hbar\omega_-=\hbar\omega_L$, and $\hbar\omega_-=\hbar\omega_L$, respectively.

fields up to 10 Tesla whereas our calculations were carried out for the magnetic fields in the region more than 15 Tesla, taking into account two different effective Landau states, $n=0,1$ and $l=0,1$ only. Since the MPR peak on the lower B side shifts to the higher n or l side even in the present calculations, we might expect the present theory to reproduce their experimental results qualitatively if we take into account the electronic transitions up to the second excited levels and obtain the MPR conditions valid under the magnetic fields up to 10 Tesla. The shift of the MPR peaks in the conductivity seen in Fig. 2 is represented in Fig. 4, as a function of the relative strength of the confining potential parameters for a fixed tilt angle θ. It is shown in the figure that, for a fixed value of ω_1 at a specific angle, the peaks in the low field and the middle field side of the magnetic field shift to the lower field side whereas the peak in the high field side of the magnetic field shifts to the higher field side, as the relative confining potential parameter ω_2/ω_1 is increased, while for a fixed value of ω_2, all three MPR peaks shift to the low field side of the magnetic field as the relative confining potential parameter ω_1/ω_2 is increased. Our present results for the latter case agree qualitatively with those of Suzuki *et al.*[17]

Other interesting features of the shift of the MPR peaks are expected according to the relative strength of the electron confinement due to the electrostatic potentials with respect to the magnetic confinement by an applied magnetic field. Their shifts for strong and weak confinement potentials are plotted in Fig. 5, as a function of tilt angle θ, using the MPR conditions given by Eq. (17). It is clearly seen in this figure that the resonant peaks for strong confinement appear in the low field side and their angle dependence is small whereas those for weak confinement appear in the high field side and their angle dependence is larger than that for strong confinement. Moreover, the MPR peaks exhibit a similar angle dependence of the shift, as in Fig. 3. Note that, in addtion to the MPR conditions in Fig. 3, the shift of resonant peaks given by $\hbar\omega_-=\hbar\omega_L$ appears in terms of given confining potential parameters ω_1 and ω_2. For direct comparison of the MPR conditions presented by some authors, the shift of resonant peaks given by $\hbar\omega_+=\hbar\omega_L$ as an example is represented in Fig. 6 as a function of tilt angle according to the confinement strength, where the confining potential parameters were, respectively, taken as $0.1\omega_c$ and $0.5\omega_c$ for weak confinement and $2\omega_c$ and $5\omega_c$ for strong confinement as a matter of convenience. As shown in Fig. 6, the present results of the angle dependence of the MPR peaks for weak confinement agree well with those of Suzuki *et al.*[17] for a Q1D quantum-wire structure modeled by the same potential wells, but they do not agree with our previous results,[16] whereas the present results for strong confinement agree qualitatively with those of our previous results, but they do not agree with that of

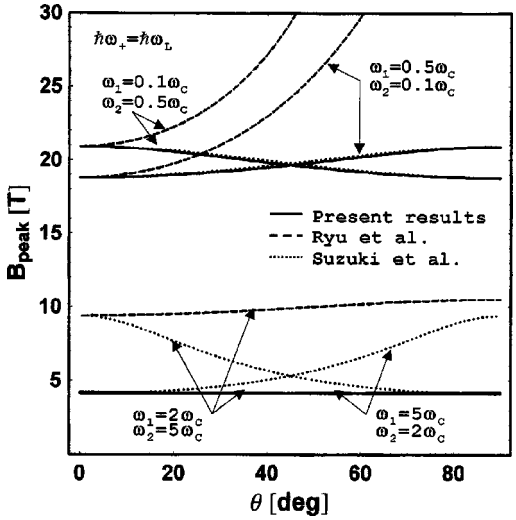

FIG. 6. Comparison with the existing theories for the tilt angle dependence of the resonant magnetic fields (B_{peak}), where ω_1 and ω_2 have been taken as $0.1\omega_c$ or $0.5\omega_c$ for weak confinements and as $2\omega_c$ or $5\omega_c$ for strong confinements. The solid, dashed, and dotted lines indicate the present result for $\hbar\omega_+=\hbar\omega_L$, Ryu *et al.*'s theoretical results, and Suzuki *et al.*'s theoretical results, respectively.

Suzuki *et al.* The difference between the present result and their results[16,17] is due to the neglect of the coupling Hamiltonian term $\sim B_x B_z xz$ in Eq. (1) or Eq. (2).

Let us turn to feature (iii) for the height and width of the MPR peaks seen in Figs. 1 and 2. The height and width of the MPR peaks seen in Figs. 1 and 2 can be explained by Eq. (14). The height of MPR peaks is influenced by amplitude factors $(\sqrt{m^*\omega_-/\tilde{m}^*\omega_+}\,\omega_z^2/\omega_+^3\{1-\exp[-\beta\hbar\omega_+]\}$ and/or $\sqrt{m^*\omega_+/\tilde{m}^*\omega_-}\,\omega_x^2/\omega_-^3\{1-\exp[-\beta\hbar\omega_-]\})$, in addition to the Lorentzian spectrum function. Figure 7 shows the variation of the heights of MPR peaks in Fig. 1 as a function of the tilt angle of applied magnetic field. It is seen clearly in this figure that their heights increase as the tilt angle increases. The increase is given in terms of the amplitude factors and it is understood that the spikes on the curve arise from the Lorentzian spectrum function. The variation of the heights of MPR peaks in Fig. 2 is presented in Fig. 8 as a function of the relative strength of confining potential parameters. The changes of their heights in this figure can be understood by the amplitude factors, as in Fig. 7. When the relative strengths of the confining potential parameters increase, the heights of all three MPR peaks decrease, which agrees qualitatively with the experimental results of Brummell *et al.*[6] for Q2D electronic systems and with the theoretical results of Suzuki *et al.*[17] The width of MPR peaks is mainly determined by the Lorentzian spectrum function in Eq. (14) through the behavior of $\tilde{\Gamma}$, which appears in terms of the collision broadening due to the electron-phonon interaction and plays the role of the width in the spectral line shape.[27] Therefore, the width broadening of MPR peaks shown in Figs. 1 and 2 can be understood by the terms including $(\hbar\omega_\pm)^2$ in Eq. (14). Figure 9 shows the variation of the width of MPR peaks as a function of tilt angle. It can be seen from the figure that, as the tilt angle increases, the widths increase for $\omega_1<\omega_2$, but they decrease for $\omega_1>\omega_2$,

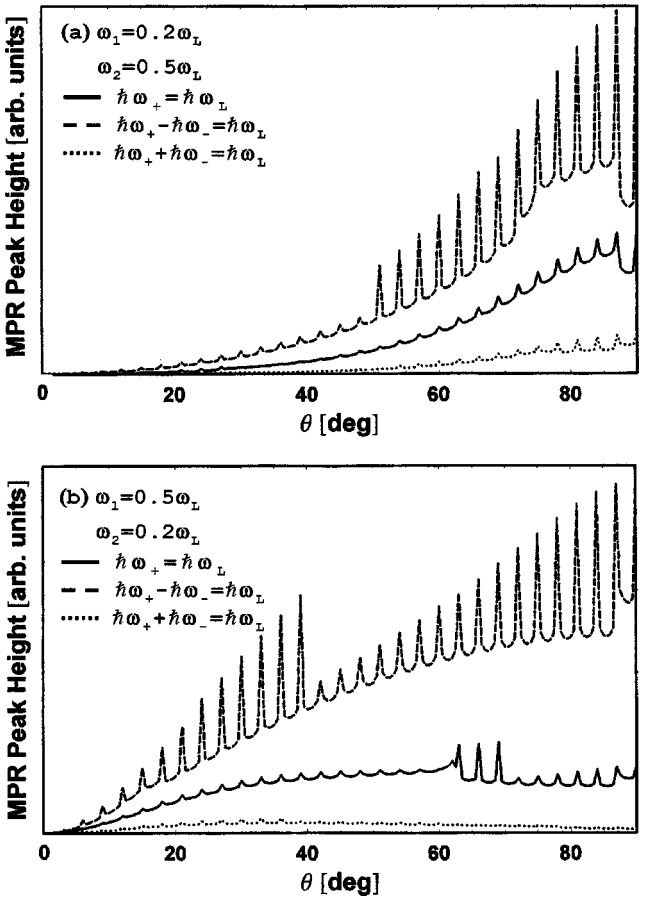

FIG. 7. Tilt angle dependence of the MPR peak heights: (a) $\omega_1=0.2\omega_L$, $\omega_2=0.5\omega_L$ and (b) $\omega_1=0.5\omega_L$, $\omega_2=0.2\omega_L$. The solid, dashed, and dotted lines indicate $\hbar\omega_+=\hbar\omega_L$, $\hbar\omega_+-\hbar\omega_-=\hbar\omega_L$, and $\hbar\omega_++\hbar\omega_-=\hbar\omega_L$, respectively.

This means that, as the tilt angle increases, the effective confinements for $\omega_1<\omega_2$ are tighter and electrons are further confined in the narrow region, while for $\omega_1>\omega_2$ the effective confinements are looser and electrons are confined in the wide region. As a result, for $\omega_1<\omega_2$, the frequency of collisions between electrons and LO phonons increases and the relaxation time becomes shorter due to the collision (scattering), while for $\omega_1>\omega_2$, the frequency of collisions decreases and the relaxation time becomes longer. Our theoretical results for the angle dependence of MPR width for $\omega_1<\omega_2$ agree qualitatively with the experimental results of Brummell *et al.*[6] for Q2D electronic systems and with the theoretical results of Suzuki *et al.*,[17] which is unlike the case of $\omega_1>\omega_2$. The variation of the widths of MPR peaks in Fig. 2 is presented in Fig. 10 as a function of the relative strength of confining potential parameters. In this figure, we can see that the width broadening is increasing with increasing one of the confining potential parameters. This means that, as one of the confining potentials increases, the effective confinements are tighter and electrons are further confined in the narrow region, as in the angle dependence of width for $\omega_1<\omega_2$. Our theoretical results for the strength dependence of confining potential parameters of MPR width agree qualitatively with the experimental results of Brummell *et al.*[6] for Q2D electronic systems and with the theoretical results of Suzuki *et al.*[17] for Q1D systems.

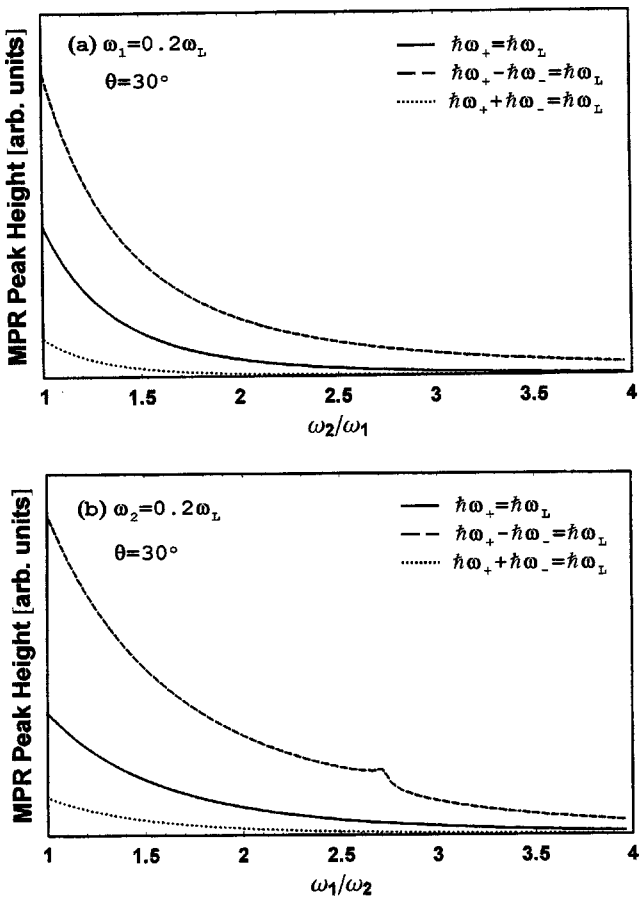

FIG. 8. Relative confining potential strength dependence of the MPR peak heights at a fixed angle $\theta=30°$: (a) $\omega_1=0.2\omega_L$ and (b) $\omega_2=0.2\omega_L$. The solid, dashed, and dotted lines indicate $\hbar\omega_+=\hbar\omega_L$, $\hbar\omega_+-\hbar\omega_-=\hbar\omega_L$, and $\hbar\omega_++\hbar\omega_-=\hbar\omega_L$, respectively.

Through all figures presented here, we can summarize the physical characteristics of the MPR line shape as follows: for the symmetric quantum wire, there are no shifts in MPR peaks as the tilt angle is increased, while for the asymmetric quantum wire, the shift of MPR peaks and the change of their amplitude and width are sensitive to the tilt angle. The angular dependences of the shift of MPR peaks and of the change of their width for $\omega_1>\omega_2$ are contrary to those for $\omega_1<\omega_2$. As one of the confining potential parameters (ω_1 and ω_2) is increased, the MPR peaks in the low field and the middle field side of the magnetic field shift to the lower field side, whereas the peak in the high field side of the magnetic field shifts to the higher field side or the lower field side depending on the condition $\omega_1<\omega_2$ or $\omega_1>\omega_2$. In addition, the widths of MPR peaks are increased, but their peak heights decrease.

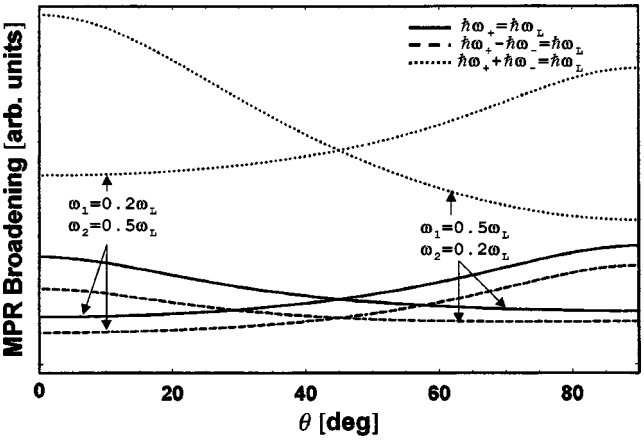

FIG. 9. Tilt angle dependence of the MPR widths for $\omega_1=0.2\omega_L$, $\omega_2=0.5\omega_L$ and $\omega_1=0.5\omega_L$, $\omega_2=0.2\omega_L$. The solid, dashed, and dotted lines indicate $\hbar\omega_+=\hbar\omega_L$, $\hbar\omega_+-\hbar\omega_-=\hbar\omega_L$, and $\hbar\omega_++\hbar\omega_-=\hbar\omega_L$, respectively.

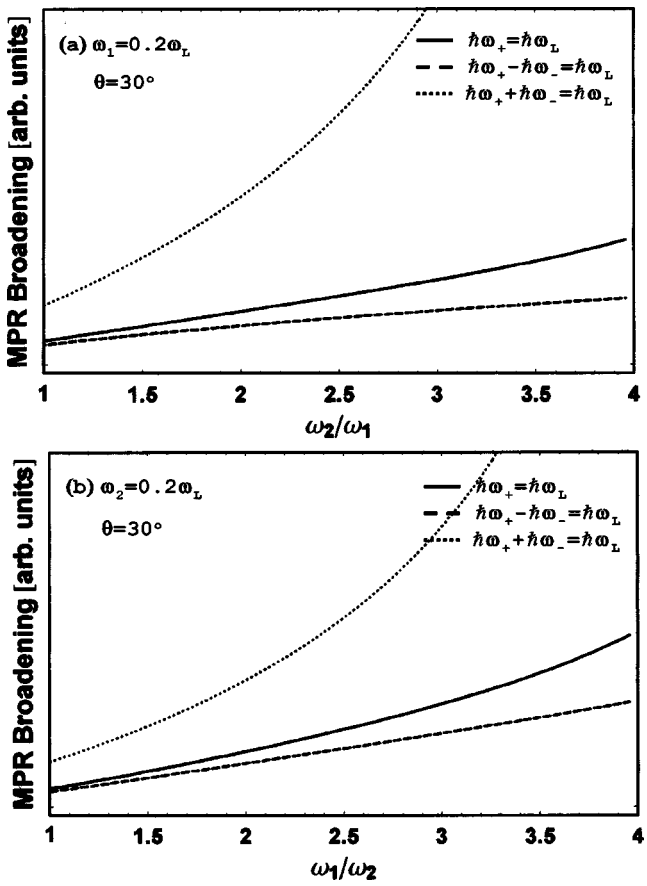

FIG. 10. Relative confining potential strength dependence of the MPR widths at a fixed angle $\theta=30°$: (a) $\omega_1=0.2\omega_L$ and (b) $\omega_2=0.2\omega_L$. The solid, dashed, and dotted lines indicate $\hbar\omega_+=\hbar\omega_L$, $\hbar\omega_+-\hbar\omega_-=\hbar\omega_L$, and $\hbar\omega_++\hbar\omega_-=\hbar\omega_L$, respectively.

V. CONCLUSIONS

In conclusion, we have derived the conductivity σ_{yy} for Q1D electronic systems subjected to crossed electric ($\mathbf{E}||\hat{y}$) and magnetic fields $\mathbf{B}=(B_x,0,B_z)$, based on a simple model of parabolic confining potentials, and we obtained the MPR conditions in the quantum limit condition, as a function of the strength (B) and tilt angle (θ) of the applied magnetic field ($\mathbf{B}$) as well as the strength of the parabolic potential parameters (ω_1 and/or ω_2). With the MPR conditions, we have investigated the physical characteristics of the MPR effects, according to the tilt angle of the applied magnetic field and the relative strength of the confining potential parameters, in such Q1D systems. In particular, we have studied the qualitative features of the MPR effects and their physical origin, and we compared with the existing theoret-

ical results because we are not aware of any relevant experimental work on MPR on the dependence of the tilted magnetic field on the σ_{yy} for Q1D electronic systems. Some comments related to this work should be made as follows. (i) Our theoretical results are based on a model of parabolic confining potential. For usual heterostructures it is well known that the confinement potential in the z direction is far from being parabolic and is often approximated by a triangular potential.[12,14] For direct comparison with experiments, realistic modeling with the correct confinement potential should be required. We believe, however, that utilizing a model with a parabolic confinement is good enough to extract the essential physics of MPR effects in Q1D electronic systems in tilted magnetic fields. (ii) The single-particle picture has been used throughout this work, and thus the electron-electron interactions have been ignored. The effect of electron-electron interaction can be taken into account approximately by replacing the electron-phonon interaction included in Eq. (9) by a screened electron-phonon interaction $iD\hbar^{1/2}/(2\rho\omega_L V)^{1/2}[1+\lambda^2(\mathbf{q})/q^2]$,[17] since the inverse screening length $\lambda(\mathbf{q})$ depends on the electron density n_e, which in general depends on temperature T and the magnetic field $\mathbf{B}$. Therefore, we would expect the screening to be significant only if the electron density n_e exceeds a critical value $n_{cr}(T,\mathbf{B})$. In this case, the effects of electron-electron scattering would be significant, and the relaxation rate will be changed and the MPR line shape as well as the MPR linewidth would be affected by electron-electron scattering. (iii) Any modification of the electron-phonon interaction brought about by the confinement of phonons (we used the interaction for bulk phonons) has not been taken into consideration. A possible influence of the modification can be included[28] in the electron-phonon interaction in Eq. (9). Although such modifications would be expected to affect the MPR line shape considerably, as in the electron-electron scattering case, they are not expected to change the physical characteristics of MPR effects, such as the appearance of subsidiary MPR peaks and the shift of these MPR peaks.

Despite the above shortcomings of the theory, we believe that the simple model we present captures qualitatively the essential physics on MPR in Q1D electronic systems brought about by the electron confinement due to the electrostatic potentials and the magnetic confinement by tilting a magnetic field. We hope that new experiments will test the validity of our prediction.

ACKNOWLEDGMENTS

One of the authors (J.Y.R.) would like to thank Professor A. Suzuki for sending him a reprint related to this work. This research was supported in part by the LG Foundation, Korea and in part by the Texas Center for Superconductivity at the University of Houston, Texas.

[1] D. C. Tsui, Th. Englert, A. Y. Cho, and A. C. Gossard, Phys. Rev. Lett. **44**, 341 (1980).
[2] G. Ploner, J. Smoliner, G. Strasser, M. Hauser, and E. Gornik, Phys. Rev. B **57**, 3966 (1998).
[3] P. Vasilopoulos, Phys. Rev. B **33**, 8587 (1986).
[4] N. Mori, K. Taniguchi, C. Hamaguchi, S. Sasa, and S. Hiyamizu, J. Phys. C **21**, 1791 (1988).
[5] M. A. Brummell, D. R. Leadley, R. J. Nicholas, M. A. Hopkins, J. J. Harris, and C. T. Foxon, Phys. Rev. Lett. **58**, 77 (1988).
[6] M. A. Brummell, D. R. Leadley, R. J. Nicholas, J. J. Harris, and C. T. Foxon, Surf. Sci. **196**, 451 (1988).
[7] D. R. Leadley, R. J. Nicholas, J. Singleton, W. Xu, F. M. Peeters, J. T. Devreese, J. A. A. J. Perenboom, L. van Bockstal, F. Herlach, J. J. Harris, and C. T. Foxon, Phys. Rev. Lett. **73**, 589 (1994).
[8] P. Vasilopoulos, M. Charbonneau, and C. M. Van Vliet, Phys. Rev. B **35**, 1334 (1987).
[9] P. Warmenbol, F. M. Peeters, and J. T. Devreese, Phys. Rev. B **39**, 7821 (1989); **37**, 4694 (1988).
[10] N. Mori, H. Murata, K. Taniguchi, and C. Hamaguchi, Phys. Rev. B **38**, 7622 (1988).
[11] A. Suzuki, Phys. Rev. B **45**, 6731 (1992).
[12] P. Vasilopoulos, P. Warmenbol, F. M. Peeters, and J. T. Devreese, Phys. Rev. B **40**, 1810 (1989).
[13] N. Mori, H. Momose, and C. Hamaguchi, Phys. Rev. B **45**, 4536 (1992).
[14] J. Y. Ryu and R. F. O'Connell, Phys. Rev. B **48**, 9126 (1993).
[15] G. Berthold, J. Smoliner, E. Gornik, G. Böhm, G. Weimann, T. Suski, P. Wisniewski, C. Hamaguchi, N. Mori, and H. Momose, Surf. Sci. **395**, 637 (1994).
[16] J. Y. Ryu, G. Y. Hu, and R. F. O'Connell, Phys. Rev. B **49**, 10 437 (1994).
[17] A. Suzuki and M. Ogawa, J. Phys. C **10**, 4659 (1998).
[18] G. Ihm, M. L. Falk, S. K. Noh, J. I. Lee, and S. J. Lee, Phys. Rev. B **46**, 15 530 (1992).
[19] J. Y. Ryu and S. D. Choi, Phys. Rev. B **44**, 11 328 (1991).
[20] I. S. Gradshteyn and I. M. Ryzhik, *Tables of Integrals, Series, and Products* (Academic, New York, 1965).
[21] J. Singh, *Physics of Semiconductors and Their Heterostructures* (McGraw-Hill, Singapore, 1993), p. 455.
[22] B. K. Ridley, *Quantum Processes in Semiconductors* (Clarendon Press, Oxford, 1993), p. 41.
[23] V. L. Gurevich and Yu A. Firsov, Zh. Éksp. Teor. Fiz. **40**, 198 (1961) [Sov. Phys. JETP **13**, 137 (1961)].
[24] Yu A. Firsov, V. L. Gurevich, R. V. Parfeniev, and S. S. Shalyt, Phys. Rev. Lett. **12**, 660 (1964).
[25] R. A. Stradling and R. A. Wood, J. Phys. C **1**, 1711 (1968).
[26] J. R. Barker, J. Phys. C **5**, 1657 (1972).
[27] J. Y. Ryu, Y. C. Chung, and S. D. Choi, Phys. Rev. B **32**, 7769 (1985).
[28] N. Sawaki, Surf. Sci. **170**, 537 (1986).